

## Delayed proton emission of $N = 81$ odd-odd precursors: $^{148}\text{Ho}$ , $^{150}\text{Tm}$ , and $^{152}\text{Lu}$

J. M. Nitschke, P. A. Wilmarth, and J. Gilat\*  
Lawrence Berkeley Laboratory, Berkeley, California 94720

K. S. Toth  
Oak Ridge National Laboratory, Oak Ridge, Tennessee 37831

F. T. Avignone III  
University of South Carolina, Columbus, South Carolina 29208  
(Received 22 June 1987)

Beta-delayed proton decay was observed in  $^{148}\text{Ho}$ ,  $^{150}\text{Tm}$ , and  $^{152}\text{Lu}$  for the first time. Contrary to neighboring even- $Z$   $N = 81$  isotones, the proton spectra appear structureless and statistical in nature. Proton branching ratios for the high-spin isomers in these isotopes, based on the intensity of  $\gamma$ -ray transitions in the intermediate nuclei, are  $(8 \pm \frac{1}{2}) \times 10^{-4}$ ,  $(1.2 \pm_{0.4}^{0.2}) \times 10^{-2}$ , and  $(1.5 \pm 0.7) \times 10^{-1}$ , respectively. The onset of proton emission in all three cases occurs at a proton to  $\gamma$  width ratio of about  $10^{-4}$ . Protons were found to be in coincidence with x rays,  $\gamma$  rays, and positrons. Coincident  $K$  x rays served to identify the  $Z$  of the precursor, while the  $\gamma$  rays gave quantitative information about proton decay to excited states in the daughter nuclei. By comparing the final state branching ratios with statistical model calculations, it was concluded that  $^{148}\text{Ho}$  and  $^{150}\text{Tm}$  both have isomers with probable spin values of  $1^+$  and  $6^-$ . Statistical model calculations with "standard" prescriptions for level densities and  $\gamma$  widths, and with a reduced level density parameter are compared to experiment. To reproduce the shape of the proton spectrum it was necessary to assume Gaussian-shaped Gamow-Teller  $\beta$  strength functions centered near 8 MeV excitation energy. In the course of these experiments  $\beta$ -delayed proton emission in  $^{148}\text{Er}$  was also identified.

### I. INTRODUCTION

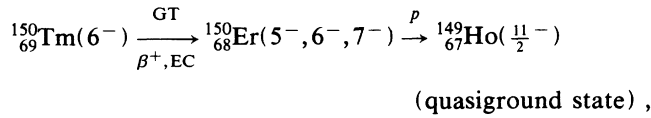
Beta-delayed proton emission is a phenomenon characteristic of nuclei near the proton drip line. In the region of  $A < 70$  delayed proton spectra are composed of discrete transitions from levels in the proton emitting nucleus (emitter) to levels in the final nucleus, usually dominated by transitions to the isobaric analog state. Levels in the emitter typically have spacings larger than the detector resolution for protons due to the relatively low level density in light nuclei. Thus, the energies and intensities of the proton lines yield a wealth of information on  $\beta$  decay to levels at high excitation energies.<sup>1,2</sup> In contrast, nuclei in the heavier mass regions, such as the rare earth elements, have level densities—at excitation energies that are sufficiently high for proton decay—in excess of  $10^3$  MeV<sup>-1</sup>. Since the resolution of solid state detectors commonly used for charged particle spectroscopy is rarely better than 10 keV, the proton spectra appear smooth and unresolved. The high level density justifies the treatment of the proton versus  $\gamma$ -ray emission process in the framework of a statistical model.<sup>3</sup> Some proton emitters near the  $Z = 50$  closed shell show a pronounced structure in their spectra which has been interpreted as Porter-Thomas fluctuations.<sup>4</sup> Subsequently, well-defined proton structures were also observed in the precursor  $^{147}\text{Dy}$ ,<sup>5,6</sup> whose  $\beta$ -decay daughter  $^{147}\text{Tb}$ , is just one proton removed from the doubly magic nucleus  $^{146}\text{Gd}$ . This was at first attributed to the reduced level density associated with both the  $N = 82$  shell and  $Z = 64$  subshell closures,

but it was later shown that the relevant shell is  $N = 82$  since the sharp structure was also observed in  $^{149}\text{Er}$  (Refs. 7–9) and  $^{151}\text{Yb}$ ,<sup>10</sup> where the daughter nuclei,  $^{149}\text{Ho}$  and  $^{151}\text{Tm}$ , are three and five protons removed from  $Z = 64$ , respectively.

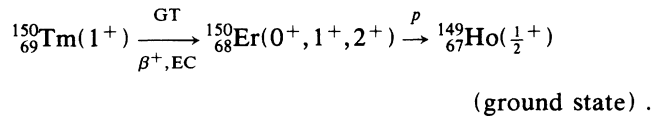
The aim of the present investigation was to study  $N = 81$  isotones with odd- $Z$  numbers to determine whether a qualitative change in the spectra compared to even- $Z$ ,  $N = 81$  isotones would occur. Such a change is expected for the following reasons: (1) in an odd-odd precursor such as  $^{150}_{69}\text{Tm}$ , an unpaired proton decays into a neutron, leaving the  $p$ -emitting nucleus in a state of relatively high excitation energy reflected by a Gamow-Teller (GT) resonance at about 7 MeV [see Fig. 1(a)], while in an even-odd precursor such as  $^{151}_{70}\text{Yb}$ , a proton pair has to be broken, lowering the GT resonance in the  $\beta$ -strength function  $S_\beta$ , by about twice the pairing gap energy to about 5 MeV [Fig. 1(b)]; and (2)  $\beta$ -decaying odd-odd precursors populate even-even emitters with large proton binding energies  $S_p$  ( $\sim 3$  MeV in  $^{150}_{68}\text{Er}$ ), while even-odd precursors populate odd-even emitters with small proton binding energies ( $\sim 0.4$  MeV in  $^{151}_{69}\text{Tm}$ ). The combined effect is a 2.5–3.5 MeV shift in the mean effective excitation energy from which protons are emitted, which corresponds to a change in level density by about 2 orders of magnitude.

Both odd-odd and even-odd  $N = 81$  precursors have  $\beta$ -decaying low- and high-spin isomers, but the final nucleus is very different in the two cases. In the odd-odd case the final nucleus (odd-even) has two nearly degenerate

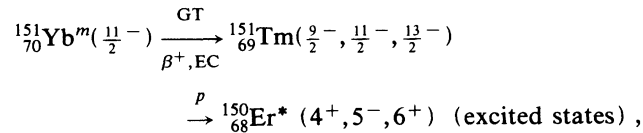
ground states with  $J^\pi = \frac{1}{2}^+$  and  $\frac{11}{2}^-$ , creating two nearly parallel paths for  $\beta$ -delayed high- and low-spin proton decay [see Fig. 1(a)]. For example, one can write symbolically for the high-spin decay of  $^{150}\text{Tm}$ :



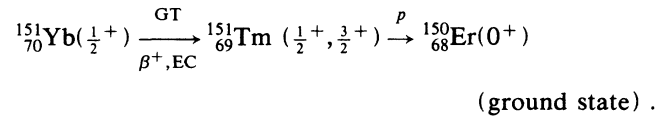
and for the low-spin decay of  $^{150}\text{Tm}$ :



Since the energetics for the two paths are the same within a few hundred keV, the high- and low-spin branches are not easily distinguished experimentally. In contrast, the even-even  $N=82$  final nucleus for an even-odd  $N=81$  precursor [see Fig. 1(b)] has a  $0^+$  ground state, and higher spin states at 1.5–3.0 MeV excitation. This leads to different energetics for the low- and high-spin decay branches [see Fig. 1(b)]. For example, in the case of  $^{151}\text{Yb}$  the high-spin decay can be written as



and the low-spin decay as



Since the excitation energies in  $^{151}\text{Tm}$  are different, the two branches can be distinguished experimentally by the different EC to positron ratios in the decay feedings. We showed in Ref. 10 that the low-spin branch is associated with proton decay from low level density and low excitation energy states in the emitter, giving rise to the structured proton spectrum typical for the even-odd  $N=81$  precursors  $^{147}\text{Dy}$ ,  $^{149}\text{Er}$ , and  $^{151}\text{Yb}$ . In the same paper it was shown that the high-spin branch gave rise to a statistical spectrum originating from high excitation energies and high level densities in the emitter. This high-spin branch in even-odd  $N=81$  precursors is therefore similar to the combined high- and low-spin delayed proton decay branches in odd-odd  $N=81$  precursors. We will show this to be true for the new isotope  $^{152}\text{Lu}$ , and for the delayed-proton branches in  $^{150}\text{Tm}$  and  $^{148}\text{Ho}$  observed here for the first time.

Several authors in the past have estimated the threshold for proton emission.<sup>1,11</sup> Since we have produced a series of six  $N=81$  isotones from  $^{147}\text{Dy}$  to  $^{152}\text{Lu}$ , we attempted to find a criterion that would give a consistent description of the onset of proton emission. An obvious choice for such a criterion is the ratio of the proton to  $\gamma$  decay widths  $\Gamma_p/\Gamma_\gamma$ , since these two processes are in competition with each other. This ratio is approximately

equal to  $\Gamma_p/(\Gamma_\gamma + \Gamma_p)$  because  $\Gamma_p \ll \Gamma_\gamma$  at the onset of proton emission. The proton width is related to the transmission coefficients  $T_l$  and the level density  $\rho$  through the well known relationship

$$\Gamma_p(E) = [2\pi\rho(E)]^{-1} \sum_j T_{lj}(E),$$

where the sum is taken over all initial states in the emitter and all final states in the daughter nucleus. Transmission coefficients were calculated with several sets of optical model parameters. Values of  $\Gamma_p/\Gamma_\gamma$  quoted in this paper are based on parameters given by Becchetti and Greenlees,<sup>12</sup> while the level densities  $\rho_l$  were calculated according to Dilg *et al.*<sup>13</sup> Average radiation widths  $\langle \Gamma_\gamma \rangle$  of states with spin  $J$  at excitation energy  $E_x$  were calculated according to the following formula suggested by Hardy<sup>14</sup>

$$\langle \Gamma_\gamma(E_x) \rangle = \int_0^{E_{\text{max}}} E_\gamma^3 f_{E1}(E_\gamma) \sum_{I=J-1}^{I=J+1} \frac{\rho_I(E_x - E_\gamma)}{\rho_J(E_x)} dE_\gamma,$$

where  $\rho_J$  is the density of spin  $J$  states,  $f_{E1}$  is the strength function for  $E1$   $\gamma$  decay;  $f_{E1}(E_\gamma) = 8.7 \times 10^{-8} \sigma(E_\gamma)/E_\gamma$ , and  $\sigma(E_\gamma)$  is the photoabsorption cross section in mb.

It was found empirically that the onset of proton emission is observed at a value of  $\Gamma_p/\Gamma_\gamma \approx 10^{-4}$ . The energy corresponding to this value is indicated in the proton spectra by double arrows. An equally good criterion for the six  $N=81$  isotones is  $\Gamma_p(E) \approx 10^{-5}$  eV, marked by single arrows in the proton spectra. Together these criteria give  $\Gamma_\gamma = 10^4 \times \Gamma_p = 0.1$  eV, which is equivalent to a lifetime of  $\tau_\gamma = 7 \times 10^{-15}$  s. Lifetimes of this order are associated with  $E1$  single-particle transitions of about 0.4 MeV or  $M1$  transitions of about 1.7 MeV (Ref. 15) which are typical energies observed in  $\gamma$ -ray cascades.

## II. EXPERIMENT

To produce the three isotopes  $^{152}\text{Lu}$ ,  $^{150}\text{Tm}$ , and  $^{148}\text{Ho}$ , targets of  $^{96}\text{Ru}$  and  $^{94}\text{Mo}$  were bombarded with beams of  $^{58}\text{Ni}$  ions from the Lawrence Berkeley SuperHILAC. Details of the compound nucleus reaction channels, target thickness, target material enrichment, laboratory projectile energy in the midplane of the target, and calculated cross sections<sup>16</sup> are given in Table I. Bombarding energies (column 7) were chosen to optimize the production of the desired isotope (column 1) *via* the reaction channel given in column 4. Heavy ion beam currents were typically in the range of  $(0.5-1.0) \times 10^{12}$  particles  $\text{s}^{-1}$ , limited by the mechanical stability of the gas-cooled  $^{96}\text{Ru}$  targets,<sup>17,18</sup> or the uncooled  $^{94}\text{Mo}$  targets. The evaporation residue recoils were stopped in a tantalum catcher operated close to its melting point ( $\sim 3000^\circ\text{C}$ ). The catcher was located inside a surface ionization source. After diffusing out of the catcher and being ionized, the product ions were accelerated to an energy of 50 keV and mass separated in the on-line isotope separator OASIS.<sup>19</sup> The separator was calibrated with stable rare earth isotopes introduced into the ion source as minute quantities of the oxides. For the separation of the radioactive isotopes, small corrections to the mass values of the stable

TABLE I. Experimental parameters for the production of the  $\beta$ -delayed proton precursors  $^{152}_{71}\text{Lu}$ ,  $^{150}_{69}\text{Tm}$ , and  $^{148}_{67}\text{Ho}$ .

Isotope	Target	Projectile	Reaction channel	Target thickness (mg/cm <sup>2</sup> )	Target enrichment (%)	Projectile lab. energy target center (MeV)	Calculated cross section at projectile energy (mb)
$^{148}_{67}\text{Ho}$	$^{94}_{42}\text{Mo}$	$^{58}_{28}\text{Ni}$	3pn	2.0	93.9	257	80
$^{150}_{69}\text{Tm}$	$^{96}_{44}\text{Ru}$	$^{58}_{28}\text{Ni}$	3pn	1.6	96.5	267	20
$^{152}_{71}\text{Lu}$	$^{96}_{44}\text{Ru}$	$^{58}_{28}\text{Ni}$	pn	1.5	96.5	244	0.4

isobars were applied to take into account mass changes within an isobaric chain for nuclei far from stability. A single isobaric chain was selected at the focal plane of the separator and transported ionoptically to a shielded, low background spectroscopy laboratory. Here the 50-keV ions were implanted in a 50- $\mu\text{m}$  Mylar tape and transported within 180 ms to an array of detectors consisting of a Si  $\Delta E$ - $E$  particle telescope, a hyperpure Ge detector [0.7 keV full width at half maximum (FWHM) resolution at 122 keV], two  $n$ -type Ge detectors with relative efficiencies of 24% (1.9 keV FWHM resolution at 1332 keV) and 52% (2.4 keV FWHM resolution at 1332 keV), and a thin plastic  $\Delta E_{\beta}$  detector. A scale drawing of the detector arrangement is shown in Fig. 1 of Ref. 20. Coincidences between protons, x rays,  $\gamma$  rays, and positrons were recorded event by event on magnetic tape for subsequent off-line analysis. After the arrival of a fresh sample of isotopes at the detector array a quartz controlled clock was started that tagged all events with a relative time signal for half-life information. Appropriate counting time

intervals were chosen, taking into account the known or expected half-lives. In the cases of  $^{152}\text{Lu}$ ,  $^{150}\text{Tm}$ , and  $^{148}\text{Ho}$  the tape cycles were 4, 8, and 16 s, respectively. A new batch of collected isotopes was supplied by the computer controlled tape system at the conclusion of each counting interval. Concurrent with the event-by-event data acquisition, time resolved spectroscopy singles data were taken with the 24%  $\gamma$ -ray detector. Counting intervals for the singles measurements were typically divided into eight equal time bins.

Energy and efficiency calibrations of the Ge detectors were carried out with standard sources; x-ray and  $\gamma$ -ray efficiencies were linked to the efficiency of the particle telescope *via* the  $\alpha/\gamma$  decay of  $^{241}\text{Am}$ . The relative efficiencies of the particle telescope and the 24%  $\gamma$  detector were also checked during the  $^{152}\text{Lu}$  and  $^{150}\text{Tm}$  experiments by comparing the  $\alpha$ -decay strengths of  $^{152}\text{Er}$  and  $^{150}\text{Dy}$  relative to photon intensities of known  $\gamma$ -ray transitions in  $^{152}\text{Ho}$  and  $^{150}\text{Tb}$ . The  $\alpha$  branches of  $^{152}\text{Er}$  and  $^{150}\text{Dy}$  were then deduced to be  $86 \pm 4\%$  and  $39 \pm 5\%$ , respectively, in agreement with values adopted in Nuclear Data Sheets.<sup>21,22</sup> These checks are important for judging the reliability of the proton branching ratio measurements. The detection efficiency of the thin (1 mm)  $\Delta E_{\beta}$  plastic detector for positrons was calibrated with the lowest-energy proton line in the  $^{151}\text{Yb}$  spectrum<sup>10</sup> which is predominantly populated by positron decay. A small correction for the EC contribution was applied, and a cross check was carried out by observing the 511 keV annihilation radiation from the positrons in the appropriate detectors.

### III. RESULTS

#### A. Decay of $^{148}_{67}\text{Ho}_{81}$ to $^{147}_{65}\text{Tb}_{82}$

The high-spin isomer of  $^{148}\text{Ho}$  was first observed by Toth *et al.*<sup>23</sup> *via* its decay to the first  $3^-$  state of  $^{148}\text{Dy}$  at 1688 keV. Its half-life was determined to be  $9 \pm 1$  s. Subsequently, Nolte *et al.*<sup>24</sup> reported the discovery of the low-spin ( $1^+$ ) isomer with a half-life of  $2.2 \pm 1.1$  s. Only three  $\gamma$  rays following the decay of  $^{148}\text{Ho}$  were known at the time, with most of the  $\beta$  decay of the low-spin isomer proceeding directly to the  $^{148}\text{Dy}$  ground state. In the meantime, a more detailed study<sup>25</sup> of the  $^{148}\text{Ho}$   $\beta$  decay has been carried out, including the observation of at least 40 transitions.

With the isotope separator calibrated at  $A = 148$  using the stable isotope  $^{148}\text{Nd}$ , the  $\Delta E$ - $E$  particle telescope registered the proton spectrum of Fig. 2. Figure 3(a) shows the decay of these protons from which a single com-

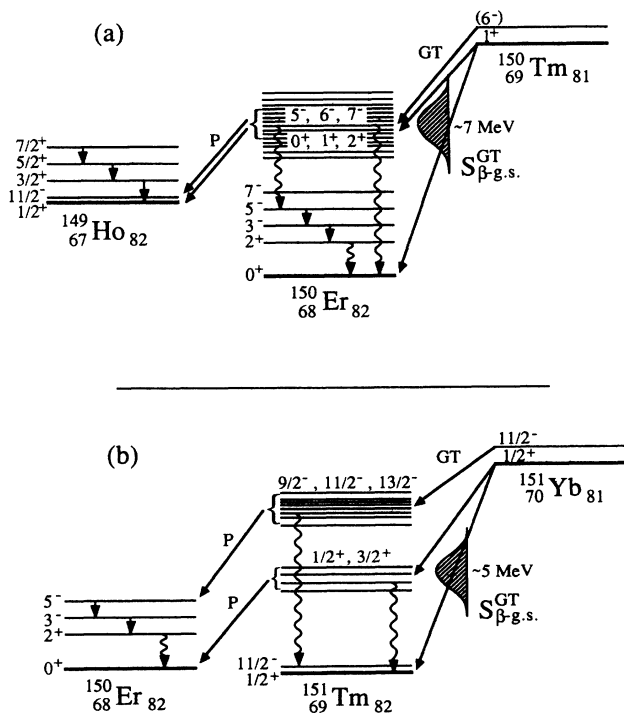


FIG. 1. Schematic representation of  $\beta$ -delayed proton decay in (a) odd- $Z$  and (b) even- $Z$   $N = 81$  precursors (see text).

ponent half-life of  $8.2 \pm 0.6$  s was derived. Only  $3.4 \pm 0.8$  % of all protons were in coincidence with positrons; the remainder followed electron capture, which gave rise to strong  $K$  x-ray peaks in the proton coincident x-ray spectrum shown in Fig. 4(a). The identification of the observed  $K$  x rays and the mass determination from the separator unambiguously established the precursor as  $^{148}\text{Ho}$ . In addition to the Dy x-ray lines, two peaks in Fig. 4(a) were identified as Ho  $K_{\alpha 1}$  and Ho  $K_{\beta 2}$  x rays, indicating that some of the delayed protons were due to a previously unknown  $\beta$ -delayed proton branch in  $^{148}\text{Er}$ . This was confirmed by the presence of a 72-keV  $\gamma$  ray [Figs. 4(a) and (b)] which belongs to the known transition between the first excited  $\frac{3}{2}^+$  state and the  $\frac{1}{2}^+$  ground state of  $^{147}\text{Dy}$ .<sup>26</sup> The observation of  $^{148}\text{Er}$  in this experiment is consistent with a calculated<sup>16</sup> cross section of 9 mb compared to that of 80 mb for  $^{148}\text{Ho}$ , and with the expected similar ionization efficiencies based on the first ionization potentials. The half-life of the proton activity,  $8.2 \pm 0.6$  s, although shorter than the value of  $9.7 \pm 0.3$  s measured<sup>25</sup> for the high-spin isomer of  $^{148}\text{Ho}$ , indicates that this isomer is the principal contributor to the  $\beta$ -delayed proton spectrum. The remaining discrepancy may be due to admixtures from  $^{148}\text{Ho}$  low-spin,  $2.2 \pm 1.1$  s,<sup>24</sup> and  $^{148}\text{Er}$ ,  $4.4 \pm 0.2$  s,<sup>25</sup> decays. The similar magnitudes of the half-lives and limited counting statistics did not allow a reliable decomposition of the proton decay curve into three components. Under the assumption that the  $^{148}\text{Ho}$  decay is dominated by the high-spin isomer (see below), a two component decay analysis with fixed half-lives (4.4 s for  $^{148}\text{Er}$  and 9.7 s for  $^{148}\text{Ho}$ ) was carried out. The result, which gave a slightly improved fit compared to the single component analysis and is shown as the curve through the data points [Fig. 3(a)], suggested a  $17 \pm 6$  % admixture of  $^{148}\text{Er}$ . This was confirmed by a

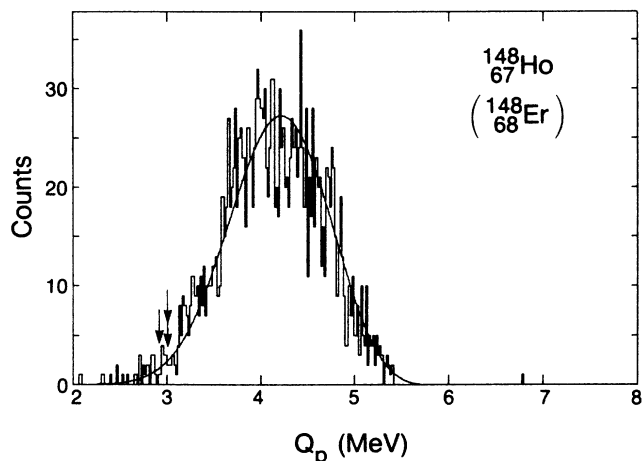


FIG. 2. Proton spectrum from Ho and Er decays observed with the  $\Delta E$ - $E$  particle telescope at mass 148. The proton decay energy  $Q_p$  is calculated as the sum of the experimental proton energy and the recoil energy. A single arrow marks the energy at which  $\Gamma_p = 10^{-5}$  eV; a double arrow indicates where  $\Gamma_p/\Gamma_\gamma = 10^{-4}$ . The smooth curve is the result of a statistical model calculation for the  $^{148}\text{Ho}$  high-spin isomer only (see text), normalized to the total number of observed protons.

careful analysis of the x-ray intensities [Fig. 4(a)] which yielded an  $^{148}\text{Er}$  admixture of  $22 \pm 5$  %. These calculations were carried out under the assumption that the  $EC/\beta^+$  ratios integrated over the proton spectrum were the same for  $^{148}\text{Ho}$  and  $^{148}\text{Er}$ . The measured energies of the proton coincident  $K_\alpha$  x rays were 47.5 and 45.9 keV, in agreement with the accepted average  $K_\alpha$  energies of 47.3 and 45.7 keV for Ho and Dy, respectively.

As discussed in the Introduction, there exists a "favored decay path" from the  $6^-/1^+$  states of  $^{148}\text{Ho}$  to the  $h_{11/2}/s_{1/2}$  quasidegenerate ground states of the daughter nucleus  $^{147}\text{Tb}$ .<sup>27</sup> Along this path protons can be emitted with low values of angular momentum, hence reducing the centrifugal barrier. For this reason, it is not surprising that only about 10% of the observed protons were in coincidence with  $\gamma$  rays from excited states in  $^{147}\text{Tb}$  [Fig. 4(b)]. After taking into account  $\gamma$ -ray efficiencies, losses due to conversion and summing, the proton decay branches  $b$ , feeding levels in  $^{147}\text{Tb}$  were:  $b(g_{7/2}) = 7 \pm 4$  %,  $b(d_{5/2}) = 1 \pm 4$  %,  $b(d_{3/2}) = 3 \pm 5$  %, and  $b(s_{1/2}, h_{11/2}) = 89 \pm 20$  %. Even though the limited statistical accuracy precluded a detailed analysis, the small branch to the first excited state ( $d_{3/2}$ ) indicates that the contribution of the  $^{148}\text{Ho}$   $1^+$  precursor state to the proton spectrum is small.

It was possible to measure the proton branching ratio for the  $^{148}\text{Ho}$  high-spin isomer by comparing the number of observed protons  $N_p$  (assuming a 20% correction for  $^{148}\text{Er}$ ), with the number of  $3^- \rightarrow 0^+$  plus  $2^+ \rightarrow 0^+$  transi-

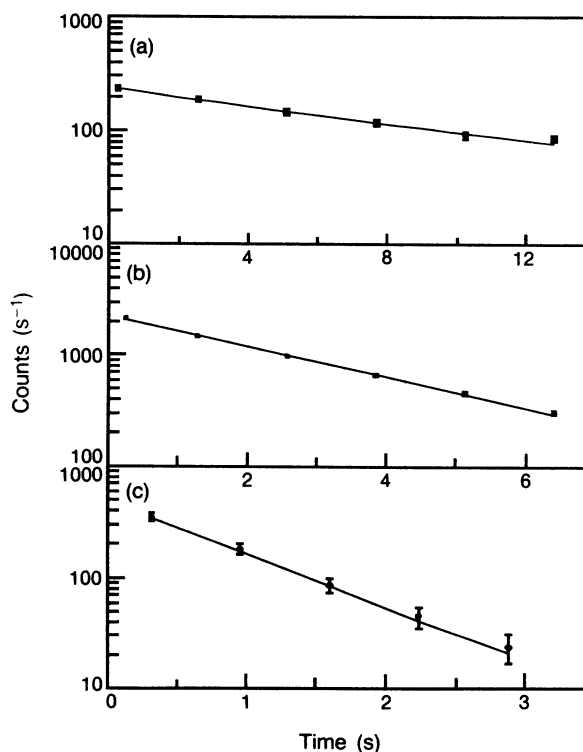


FIG. 3. (a) Decay of the proton activity at a mass separator setting of  $A = 148$  during a tape cycle of 16-s duration, (b) the same for  $A = 150$  and a tape cycle of 8-s duration, and (c) the same for  $A = 152$  and a tape cycle of 4-s duration.

tions  $N_\gamma$ , in the emitter. This ratio  $N_p/N_\gamma$  was measured to be  $(8_{-2}^{+1}) \times 10^{-4}$ . The positive error is the statistical uncertainty while the negative error also includes conservative estimates of the contribution from the low-spin ( $1^+$ ) isomer to the number of protons and the reduction of the observed  $\gamma$ -ray intensities from summing in the close counting geometries.

It is of interest to compare the observed proton spectral shape, proton branching ratio, and final state branching ratios with statistical model calculations, but efforts in this mass region are hampered by the difficulties of calculating  $\beta$ -strength functions for both the low- and high-spin states of the precursor. There are also no measurements available in this region, except for  $^{147}\text{Dy}^{m,28}$ . This makes it difficult to compare, for instance, experimental proton branching ratios with calculations. Despite the lack of information on  $\beta$ -strength functions an attempt was made to reproduce the observed proton spectrum with a statistical model calculation. Several changes over an earlier model<sup>3</sup> were already mentioned in the discussion of the proton emission threshold and the  $\Gamma_p/\Gamma_\gamma$  ratio. For the  $^{148}\text{Ho}$  high-spin isomer, the  $\beta$ -strength function was represented by a single Gaussian with a centroid  $E_0$  and a width parameter  $\sigma$ , based on the assumption that the shape of the GT resonance might be similar to that observed for  $^{147}\text{Dy}^{m,28}$ . Values for  $Q_{\text{EC}}$  of  $^{148}\text{Ho}$  and the proton separation energy  $S_p$  in  $^{148}\text{Dy}$  were obtained from Refs. 29 and 30, respectively. The  $6^-$  state was assumed to lie 0.1 MeV above the  $1^+$  ground state, and  $E_0$  and  $\sigma$  were varied until the best fit to the shape of the experimentally observed proton spectrum was obtained.

The final result of the statistical model calculation for  $^{148}\text{Ho}$ , shown in Fig. 2 as a smooth curve, was obtained

with the following set of parameters:  $E_0=8.4$  MeV,  $\sigma=0.825$  MeV,  $Q_{\text{EC}}=10.0$  MeV, and  $S_p=4.31$  MeV. The calculated proton branching ratio is  $P_p=1.1 \times 10^{-3}$  in agreement with the experimental value, and the relative branches to levels in  $^{147}\text{Tb}$  are:  $b(g_{7/2})=2.3\%$ ,  $b(d_{5/2})=1.7\%$ ,  $b(d_{3/2})=0.8\%$ , and  $b(h_{11/2})=94.5\%$ . Considering the difficulties inherent in the measurements of absolute proton branching ratios and the weak excited state feeding, the good agreement between experiment and calculation confirms our understanding of the  $^{148}\text{Ho}(6^-)$   $\beta$ -delayed proton decay.

Interpretation of the observed  $^{148}\text{Er}$   $\beta$ -delayed proton decay is simplified by the precursor  $0^+$  ground state and the nonexistence of a long-lived high-spin isomer. A statistical model calculation for  $^{148}\text{Er}$  predicts that the first excited  $\frac{3}{2}^+$  state of  $^{147}\text{Dy}$  at 72 keV should be populated by proton decay with 48% probability, with the remaining 52% going to the  $\frac{1}{2}^+$  ground state. The experimental branching ratios deduced from the number of protons in coincidence with the 72-keV  $\gamma$  ray [Fig. 4] and the estimated total number of observed protons, were:  $61 \pm 24\%$  feeding the  $\frac{3}{2}^+$  level and  $39 \pm 19\%$  feeding the ground state, in agreement with the calculations.

#### B. Decay of $^{150}\text{Tm}_{81}$ to $^{149}\text{Ho}_{82}$

The isotope  $^{150}\text{Tm}$  was first identified by Nolte *et al.*<sup>31</sup> who reported a half-life of  $3.5 \pm 0.6$  s and the observation of four  $\gamma$  rays in its  $\beta$  decay to  $^{150}\text{Er}$ . A more extensive study of the  $^{150}\text{Tm}$   $\beta$  decay was published recently<sup>32</sup> and a half-life of  $2.2 \pm 0.2$  s for the  $6^-$  state of  $^{150}\text{Tm}$  was obtained. There was indirect evidence that a low-spin ( $1^+$ )

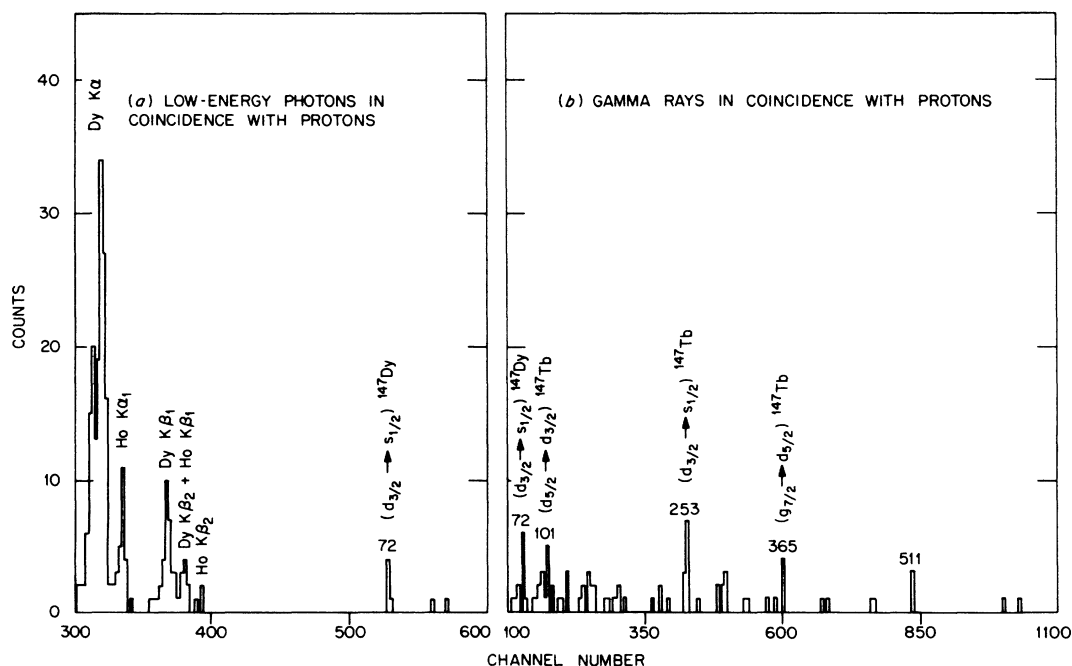


FIG. 4. (a) Low-energy photons in coincidence with protons, observed at a mass separator setting of  $A=148$ . Dysprosium and holmium  $K$  x rays are identified as well as a  $\gamma$  transition in  $^{147}\text{Dy}$ . (b) Gamma rays coincident with protons, observed at the same mass separator setting. Transitions in  $^{147}\text{Dy}$  and  $^{147}\text{Tb}$  are indicated.

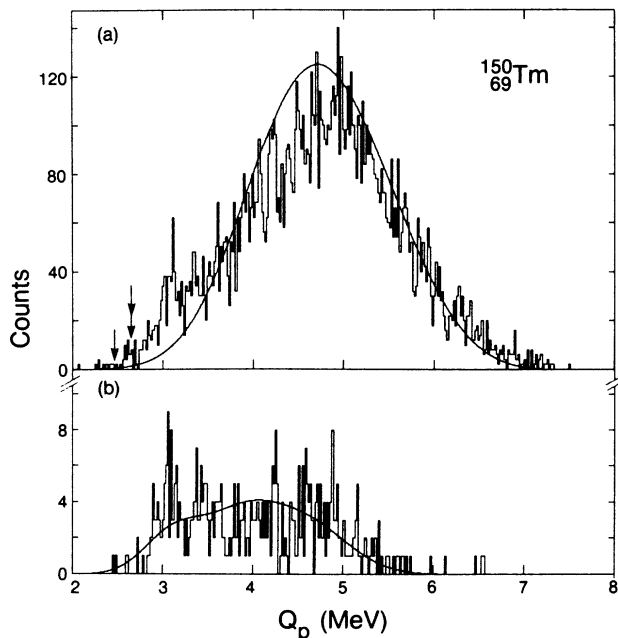


FIG. 5. (a) Proton spectrum observed at mass 150. For an explanation of  $Q_p$  and the arrows see caption of Fig. 2. The smooth curve is the result of a statistical model calculation (see text), normalized to the total number of observed protons. The contributions of the  $6^-$  and  $1^+$  states of  $^{150}\text{Tm}$  are assumed to be 80 and 20 %, respectively (see Table II and text). (b) Protons observed in coincidence with positrons. The curve overlaying the data was obtained by smoothing the proton spectrum in part (a) and multiplying it by the ratio of the Fermi functions  $f^+ / (f^+ + f^{\text{EC}})$ .

isomer in  $^{150}\text{Tm}$  was also present but no isomeric transition was observed and no half-life determined.

The proton energy spectrum and decay curve measured in our experiment for  $A=150$  is shown in Fig. 5(a), and the decay curve in Fig. 3(b). A half-life of  $2.15 \pm 0.10$  s was derived which is in agreement with the value of  $2.2 \pm 0.2$  s obtained from  $\gamma$  decay and reported in Ref. 32. Since the observed  $\gamma$  rays<sup>32</sup> originated from the high-spin ( $6^-$ ) isomer this indicates that the proton spectrum is dominated by decay from this state (unless the low-spin state has a similar half-life). Figure 5(b) shows the observed positron coincident proton spectrum. The curve in Fig. 5(b) is the smoothed, unbiased proton spectrum [Fig. 5(a)] multiplied by the ratio of the Fermi functions  $f^+ / (f^+ + f^{\text{EC}})$ . It can be seen that the observed positron coincident spectrum reflects closely the expected spectrum, except perhaps, for some excess strength at about 3 MeV proton decay energy. The x-ray spectrum coincident with EC-delayed protons is shown in Fig. 6; the observed x-ray energies of 48.7, 55.6, and 57.3 keV are in excellent agreement with accepted  $K_{\alpha}$ ,  $K_{\beta 1}$ , and  $K_{\beta 2}$  x-ray energies for Er of 48.8, 55.7, and 57.1 keV, respectively. This, in conjunction with the mass selection from the isotope separator, uniquely identifies the precursor as  $^{150}\text{Tm}$ . Contrary to the  $A=148$  experiment, there was no indication of a second group of x rays associated with another proton emitter. A possible candidate would have been  $^{150}\text{Yb}$ , but its calculated<sup>16</sup> cross section is only 0.7 mb compared to 22 mb for  $^{150}\text{Tm}$ . Another discriminating factor was the expected half-life of 0.8 s for  $^{150}\text{Yb}$ .<sup>33</sup> An isotope of such short half-life would have been strongly suppressed by the 8-s tape cycle employed

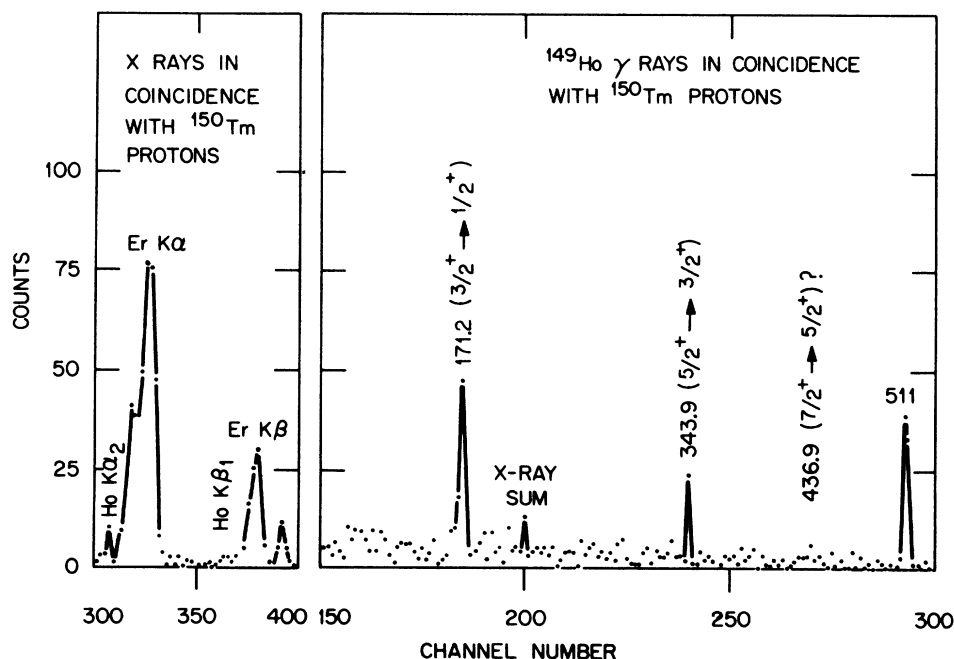


FIG. 6. Gamma rays in  $^{149}\text{Ho}$ , and  $K$  x rays measured in coincidence with  $^{150}\text{Tm}$   $\beta$ -delayed protons; additional  $\gamma$  rays were observed at 1381 and 1552 keV.

TABLE II. Experimental and calculated  $\beta$ -delayed proton branches from  $^{150}\text{Tm}$  to levels in  $^{149}\text{Ho}$ . The last column represents a mixture of 80%  $6^-$  decay and 20%  $1^+$  decay.

$J^\pi$	Levels in $^{149}\text{Ho}$		Proton branching ratios (%)		
	Energy (keV)	Experiment	Calc. $^{150}\text{Tm}(6^-)$	Calc. $^{150}\text{Tm}(1^+)$	$[0.8(6^-) + 0.2(1^+)]$
$\frac{1}{2}^+$	0	$78 \pm 4.7$	92.3	46.3	83.1
$\frac{11}{2}^-$					
$\frac{3}{2}^+$	171.5	$6.5 \pm 2.4$	1.7	41.2	9.6
$\frac{5}{2}^+$	515.4	$4.3 \pm 1.9$	1.8	11.5	3.7
$\frac{7}{2}^+$	952.1	$4.5 \pm 1.3$	2.2	1.0	2.0
$\frac{15}{2}^+ \text{a}$	1380 <sup>b</sup>	$5.4 \pm 2.7$	1.4	0.0	1.1
$\frac{15}{2}^- \text{a}$	1560 <sup>b</sup>	$1.2 \pm 1.2$	0.6	0.0	0.5

<sup>a</sup>Spin and parity assignments of these levels are uncertain; the statistical model calculations are, however, not sensitive to variations of  $\pm 1$  unit of angular momentum because of the low branching ratios.

<sup>b</sup>Reference 34.

in this experiment. From the coincident x-ray spectrum (Fig. 6) an upper limit of 5% of the Tm activity was set for the observation of a Yb proton precursor.

It can be seen in Fig. 6 that protons are observed in coincidence with several  $\gamma$  rays that can be identified as transitions in the daughter nucleus  $^{149}\text{Ho}$ . Members of the high-spin band<sup>34</sup> (not shown in Fig. 6) terminating in the  $\frac{11}{2}^-$  state and members of the low-spin band<sup>35,36</sup> decaying to the  $\frac{1}{2}^+$  state were observed. As in the case of  $^{148}\text{Ho}$  the favored decay path from the  $6^-/1^+$  states of the precursor leads to the  $\frac{11}{2}^-/\frac{1}{2}^+$  ground states of the daughter nucleus. This results in small branches to excited states in  $^{149}\text{Ho}$  and consequently in a low statistical accuracy for the observation of  $\gamma$  transitions from these states. The third column of Table II summarizes the observed relative proton branches to levels in  $^{149}\text{Ho}$ .

As was already discussed for the decay of  $^{148}\text{Ho}$ , the proton branching ratio can be obtained for a high-spin odd-odd precursor because almost all of its  $\beta$ -delayed  $\gamma$  decay proceeds *via* allowed GT transitions to high-spin states which ultimately concentrate their strength in one or two prominent transitions to the  $0^+$  ground state of the even-even emitter. In  $^{150}\text{Er}$  these transitions are the  $3^- \rightarrow 0^+$  1786.6-keV and the  $2^+ \rightarrow 0^+$  1579.0-keV  $\gamma$  rays. The ratio of the number of high-spin protons (it was assumed 80% of the observed protons are associated with the high-spin precursor as discussed below) to the number of 1787- and 1579-keV  $\gamma$  rays is  $(1.2_{-0.2}^{+0.2}) \times 10^{-2}$ . The reason for the asymmetric errors is the same as for  $^{148}\text{Ho}$  above.

Statistical model calculations were carried out to compare the experimental final state feedings with different assumptions about the precursor spin and parity. Again, because of the lack of theoretical or experimental information, the parameters of a single Gaussian distribution of the  $\beta$  strength were varied until a fit to the experimental proton spectrum was obtained. This is shown as the smooth curve in Fig. 5(a). The parameters  $E_0$  and  $\sigma$  of the  $\beta$  strength distribution, and the  $Q_{\text{EC}}$  and  $S_p$  values used in the calculation were:  $E_0 = 7.8$  MeV,  $\sigma = 1.45$

MeV,  $Q_{\text{EC}} = 11.7$  MeV, and  $S_p = 3.0$  MeV. The value for  $S_p$  was obtained from Ref. 29. The  $Q_{\text{EC}}$  value calculated from the same table was 11.4 MeV; we found it, however, necessary to increase this value to 11.7 MeV to correctly match the upper flank of the proton spectrum [Fig. 5(a)].

It should be noted that the shape of the proton spectra in  $^{148}\text{Ho}$ ,  $^{150}\text{Tm}$ , and  $^{152}\text{Lu}$  are sensitive only to the portion of the  $\beta$ -strength function covered by the proton energy range. In all three cases the statistical accuracy of the experiments is, however, sufficient to exclude constant or monotonic strength functions because they do not reproduce the shape of the spectra or the observed final state branching ratios. Since the  $\beta$ -strength distribution outside the proton decay window is not known, and some decay strength may go to lower excitation energies in the emitter (which is not included in the  $\beta$ -strength functions used in the calculations of the proton branching ratio) the calculated proton branching ratios have to be considered as *upper* limits. However, in  $^{148}\text{Ho}$ <sup>25</sup> and  $^{150}\text{Tm}$ <sup>32</sup> high spin  $\beta$  decays only levels above  $\sim 2.5$  MeV are populated and the electron capture to positron ratios indicate considerable feeding of very high-lying states.

Since the branching ratio of 1.2% is relatively large we have studied the effects of varying different parameters of the statistical model on the calculated proton branching ratio and final state feedings. Several of the parameters of the statistical model are constrained by systematics ( $Q_{\text{EC}}$  and  $S_p$ ), others by the final state branching ratios ( $J^\pi$ ), the shape of the proton spectrum ( $S_\beta$ ), or the positron coincident to total proton ratio ( $Q_{\text{EC}}$  and  $S_p$ ). The strongest influence on the proton branching ratio (without altering the agreement with other experimental results and keeping in mind that the assumed  $\beta$ -strength functions result in upper limits to the proton branching ratio with respect to variation in  $S_\beta$ ) is exhibited by the level density parameter  $a$ , and the gamma width. A reduction in the level density parameter increases the proton width in inverse proportion while a lowering of the  $\gamma$  width favors proton decay by reducing  $\gamma$  competition. We have found that in the case of  $^{150}\text{Tm}$  reducing  $a$

to 70%, or  $\Gamma_\gamma$  by a factor of 10 achieves the same effect: it raises the proton branching ratio by an order of magnitude. To distinguish between the two possible alternatives it is worth remembering that a reduced level density has already been postulated as the underlying cause for the structure in the proton spectra of the even-odd  $N=81$  precursors.<sup>8,10</sup> It therefore seems conceivable that this effect could also make itself felt in the odd-odd  $N=81$  precursors. By reducing  $a$  to 70% of the value of the “back shifted” Fermi level density,<sup>13</sup> upper limits for the proton branching ratios of 1.2 and 1.9 % were calculated for the  $6^-$  and  $1^+$  states of  $^{150}\text{Tm}$ , respectively. More detailed results of the calculations for these two states are given in Table II. Comparing the experimental final state proton branching ratios with the results for  $^{150}\text{Tm}(6^-)$  it is evident that this calculation does not reproduce the feeding to the excited states in  $^{149}\text{Ho}$  correctly; the same is true for the calculation starting with  $^{150}\text{Tm}(1^+)$ . A much better agreement with the experiment is, however, achieved with a 20% mixture of the  $1^+$  decay with 80% of the  $6^-$  decay as shown in the last column of Table II. Under these conditions, the weighted proton branching ratio is 1.3% compared to 1.2% from the experiment. From the  $6^-/1^+$  mixing ratio and the calculated  $6^-/1^+$  proton branches, the production ratio  $R$ , for the high-spin to low-spin precursors was estimated to be:  $R \approx (\frac{80}{20}) \times (\frac{1.9}{1.2}) \approx 6.3$ . This value is consistent with the high-spin selectivity of heavy ion reactions and the nonobservation of an isomeric transition. It should be mentioned parenthetically that the proton branching ratios to the final states are not very sensitive to small variations in  $Q_{\text{EC}}, S_p$ , and the beta strength function.

### C. Decay of $^{152}_{71}\text{Lu}_{81}$ to $^{151}_{69}\text{Tm}_{82}$

We previously reported<sup>20</sup> the first observation of  $^{152}\text{Lu}$  and its decay to levels of  $^{152}\text{Yb}$ . The half-life of the new isotope based on the deexcitation of levels in  $^{152}\text{Yb}$  was  $0.7 \pm 0.1$  s. From the observation of an allowed transition to a  $5^-$  level it was concluded that the spin/parity of  $^{152}\text{Lu}$  is  $4^-, 5^-,$  or  $6^-$ . Due to a low counting rate, no evidence for a low-spin isomer was seen.

The  $\beta$ -delayed proton spectrum measured at  $A=152$  is shown in Fig. 7. From the decay curve, Fig. 3(c), a half-life of  $0.6 \pm 0.1$  was extracted which is in agreement with the  $^{152}\text{Lu}$  half-life determined from the  $\gamma$ -ray data.<sup>20</sup> The small predicted production cross section ( $0.4 \text{ mb}$ )<sup>16</sup> and the short half-life resulted in low counting statistics, and consequently less information could be obtained for  $^{152}\text{Lu}$  compared to the other two odd-odd precursors discussed above. Copious amounts of  $\alpha$  particles from  $^{152}\text{Er}$  were produced *via* sequential  $\beta$  decay from  $^{152}\text{Yb}$  which was synthesized in the reaction  $^{96}\text{Ru}(^{58}\text{Ni}, 2p)$ . The ratio of  $\alpha$  particles to protons was 250:1; during data analysis this strong  $\alpha$  background was suppressed by well known  $\Delta E-E$  particle identification techniques. Only Yb  $K$  x rays were observed in coincidence with the protons which uniquely established the  $Z$  of the  $^{152}\text{Lu}$  precursor. No proton coincident  $\gamma$  rays in the daughter nucleus  $^{151}\text{Tm}$  were identified.

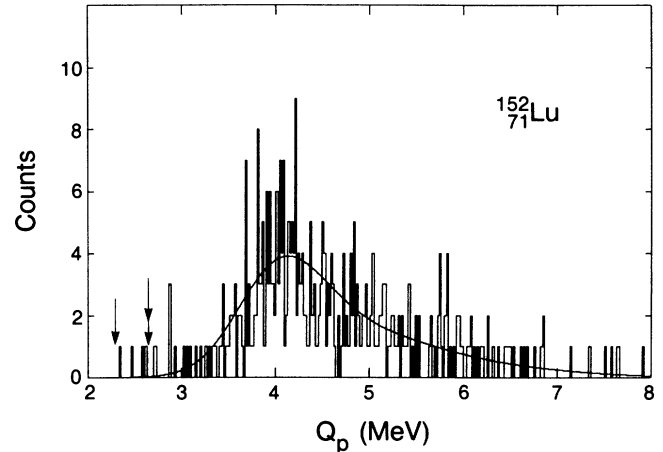


FIG. 7. Proton spectrum observed at mass 152. For an explanation of  $Q_p$  and the arrows see caption of Fig. 2. The smooth curve is the result of a statistical model calculation (see text), normalized to the total number of observed protons.

Statistical model calculations were again carried out with the reservations expressed for the other two odd-odd precursors. The  $\beta$ -strength distribution was adjusted to reproduce the wide asymmetric proton spectrum observed for  $^{152}\text{Lu}$ . Values for  $Q_{\text{EC}}=12.75$  MeV and  $S_p=2.02$  MeV were calculated from Ref. 29 and levels in  $^{151}\text{Tm}$  were taken from Ref. 37. If the assumption is made that the proton activity originates from a  $6^-$  state in  $^{152}\text{Lu}$ , an upper limit for the proton branching ratio of 1.5% is calculated; for a  $1^+$  state the upper limit is 3.1%. Experimentally, the proton branching ratio was  $(15 \pm 7)\%$  based on the observed intensity of the 1531-keV  $2^+ \rightarrow 0^+$  transition in  $^{152}\text{Yb}$ . Even though the ratio of the contributions of the high and low spin states of  $^{152}\text{Lu}$  to the proton decay is not known it is evident that the calculated proton branching ratio is substantially smaller. Calculational variations of the  $Q_{\text{EC}}$  and  $S_p$  within the uncertainties of current mass tables are unable to increase this ratio sufficiently; however, as in the case of  $^{150}\text{Tm}$  by either reducing  $\Gamma_\gamma$  a factor of 10, or reducing the level density parameter to 70% of the “back shifted” value the calculated upper limit of the proton branching ratio can be increased to 11%.

## IV. CONCLUDING REMARKS

For the first time a group of three odd-odd  $N=81$   $\beta$ -delayed proton precursors was studied. The proton spectra are distinctly different from the even-odd  $N=81$  precursors in that they resemble more closely the statistical spectra typical for heavy nuclei far from shell closures. This is interpreted as the signature of a decay path that starts with a high-spin precursor and ends in the high-spin ground state of the daughter nucleus, thereby sampling high excitation energies and level densities in the emitter. Such conditions justify the treatment of these decays in the framework of a statistical model. Lacking

detailed information about the  $\beta$ -strength functions only upper limits for the proton branching ratios can be calculated. Final state branching ratios are, however, less sensitive to the shape of  $S_\beta$  and can be used to verify assumptions about the precursor spins.

The observed half-lives for  $^{152}\text{Lu}(6^-)$  0.7 s,  $^{150}\text{Tm}(6^-)$  2.2 s, and  $^{148}\text{Ho}(6^-)/^{148}\text{Ho}(1^+)$  9.7/2.2 s are in good agreement with the predictions of the "Gross Theory of Beta Decay" (Ref. 33) of 0.5, 1.2, and 5.7 s, respectively. Half-lives obtained from proton decay agree with those obtained from  $\gamma$ -ray data taken in the same experiments; the half-life of  $^{150}\text{Tm}$  disagrees with that available in the literature.<sup>24</sup> In the course of these experiments  $\beta$ -delayed proton emission in  $^{148}\text{Er}$  was also identified.

## ACKNOWLEDGMENTS

The authors wish to thank Y. A. Ellis-Akovi, M. N. Rao, and D. M. Moltz for their participation in the data taking phase of this investigation. Technical support was provided by L. Archambault, R. Leres, and A. Wylder. The work at Lawrence Berkeley Laboratory was supported by the Director, Office of Energy Research, Division of Nuclear Physics of the Office of High Energy and Nuclear Physics of the U.S. Department of Energy under Contract No. DE-AC03-76SF00098. Oak Ridge National Laboratory is operated by Martin Marietta Energy Systems, Inc. for the U.S. Department of Energy under Contract No. DE-AC05-84OR21400.

\*On leave from Soreq Nuclear Research Center, Yavne, Israel.

<sup>1</sup>J. C. Hardy, in *Nuclear Spectroscopy and Reactions*, edited by J. Cerny (Academic Press, New York, 1974), Vol. 40C of Pure and Applied Physics, p. 417.

<sup>2</sup>J. Cerny and J. C. Hardy, *Ann. Rev. Nucl. Sci.* **27**, 333 (1977).

<sup>3</sup>P. Hornshøj, K. Wilsky, P. G. Hansen, B. Jonson, and O. B. Nielsen, *Nucl. Phys.* **A187**, 609 (1972).

<sup>4</sup>T. Elmroth, E. Hagberg, P. G. Hansen, J. C. Hardy, B. Jonson, H. Ravn, and P. Tiedemand-Peterson, *Nucl. Phys.* **A304**, 493 (1978).

<sup>5</sup>O. Klepper, T. Batsch, S. Hofmann, R. Kirchner, W. Kurcewicz, W. Reisdorf, E. Roeckl, D. Schardt, and G. Nyman, *Z. Phys. A* **305**, 125 (1982).

<sup>6</sup>R. Kirchner, O. Klepper, W. Kurcewicz, P. O. Larsson, E. Roeckl, D. Schardt, G. Nyman, and P. Tidemand-Peterson, in *Proceedings of the International Workshop on Gross Properties of Nuclei and Nuclear Excitations XI*, Hirschegg, 1983, edited by H. Feldmeier, Technische Hochschule Darmstadt Report No. AED-Conf.-75-009-000, 1983 (unpublished), p. 60.

<sup>7</sup>K. S. Toth, D. M. Moltz, E. C. Schloemer, M. D. Cable, F. T. Avignone III, and Y. A. Ellis-Akovi, *Phys. Rev. C* **30**, 712 (1984).

<sup>8</sup>D. Schardt, P. O. Larsson, R. Kirchner, O. Klepper, V. T. Koslowsky, E. Roeckl, K. Rykaczewski, P. Kleinheinz, and K. Zuber, in *Proceedings of the Seventh International Conference on Atomic Masses and Fundamental Constants, AMCO-7, Darmstadt, 1984*, edited by O. Klepper (Technische Hochschule Darmstadt, Darmstadt, 1984) (Schriftenreihe Wissenschaft und Technik), Vol. 26, p. 229.

<sup>9</sup>K. S. Toth, D. M. Moltz, E. C. Schloemer, M. D. Cable, F. T. Avignone, III and Y. A. Ellis-Akovi, in *Proceedings of the Seventh International Conference on Atomic Masses and Fundamental Constants, AMCO-7, Darmstadt, 1984*, edited by O. Klepper (Technische Hochschule Darmstadt, Darmstadt, 1984) (Schriftenreihe Wissenschaft und Technik), Vol. 26, p. 237.

<sup>10</sup>K. S. Toth, Y. A. Ellis-Akovi, J. M. Nitschke, P. A. Wilmarth, P. K. Lemmertz, D. M. Moltz, and F. T. Avignone, III, *Phys. Lett. B* **178**, 150 (1986).

<sup>11</sup>V. A. Karnaukhov, *Nukleonika* **19**, 425 (1974).

<sup>12</sup>F. D. Becchetti, Jr. and G. W. Greenlees, *Phys. Rev.* **182**, 1190 (1969).

<sup>13</sup>W. Dilg, W. Schantl, and H. Vonach, *Nucl. Phys.* **A217**, 269

(1973).

<sup>14</sup>J. C. Hardy, *Phys. Lett.* **109B**, 242 (1982).

<sup>15</sup>J. M. Blatt and V. F. Weisskopf, *Theoretical Nuclear Physics* (Wiley, New York, 1952), p. 627.

<sup>16</sup>W. G. Winn, H. H. Gutbrod, and M. Blann, *Nucl. Phys.* **A188**, 423 (1972).

<sup>17</sup>J. M. Nitschke, *Nucl. Instrum. Methods* **138**, 393 (1976).

<sup>18</sup>J. D. Molitoris and J. M. Nitschke, *Nucl. Instrum. Methods* **186**, 659 (1981).

<sup>19</sup>J. M. Nitschke, *Nucl. Instrum. Methods* **206**, 341 (1983).

<sup>20</sup>K. S. Toth, D. C. Sousa, J. M. Nitschke, and P. A. Wilmarth, *Phys. Rev. C* **35**, 310 (1987).

<sup>21</sup>C. A. Baglin, *Nucl. Data Sheets* **30**, 1 (1980).

<sup>22</sup>E. der Mateosian, *Nucl. Data Sheets* **48**, 345 (1986).

<sup>23</sup>K. S. Toth, C. R. Bingham, D. R. Zolnowski, S. E. Cala, H. K. Carter, and D. C. Sousa, *Phys. Rev. C* **19**, 482 (1979).

<sup>24</sup>E. Nolte, S. Z. Gui, G. Colombo, G. Korschinek, and K. Eskola, *Z. Phys. A* **306**, 223 (1982).

<sup>25</sup>K. S. Toth, D. C. Sousa, J. M. Nitschke, and P. A. Wilmarth, *Phys. Rev. C* **37**, 1196 (1988).

<sup>26</sup>K. S. Toth, A. E. Rainis, C. R. Bingham, E. Newman, H. K. Carter, and W.-D. Schmidt-Ott, *Phys. Lett.* **56B**, 29 (1975).

<sup>27</sup>K. S. Toth, D. M. Moltz, Y. A. Ellis-Akovi, C. R. Bingham, M. D. Cable, R. F. Parry, and J. M. Wouters, *Phys. Rev. C* **25**, 667 (1982); C. F. Liang, P. Paris, P. Kleinheinz, B. Rubio, M. Piiparinen, D. Schardt, A. Plochocki, and R. Barden, *Phys. Lett. B* **191**, 245 (1987).

<sup>28</sup>G. D. Alkhazov, A. A. Bykov, V. D. Wittmann, V. E. Starobudsky, S. Yu. Orlov, V. N. Panteleyev, A. G. Polyakov, and V. K. Tarasov, *Nucl. Phys.* **A438**, 482 (1985).

<sup>29</sup>S. Liran and N. Zeldes, *At. Data Nucl. Data Tables* **17**, 431 (1976).

<sup>30</sup>A. H. Wapstra and G. Audi, *Nucl. Phys.* **A432**, 55 (1985).

<sup>31</sup>E. Nolte, G. Colombo, S. Z. Gui, G. Korschinek, W. Schollmeier, P. Kubik, S. Gustavsson, R. Geier, and H. Morinaga, *Z. Phys. A* **306**, 211 (1982).

<sup>32</sup>K. S. Toth, D. C. Sousa, J. M. Nitschke, and P. A. Wilmarth, *Phys. Rev. C* **35**, 620 (1987).

<sup>33</sup>K. Takahashi, M. Yamada, and T. Kondoh, *At. Data Nucl. Data Tables* **12**, 101 (1973).

<sup>34</sup>J. Wilson, S. R. Faber, P. J. Daly, I. Ahmad, J. Borggreen, P. Chowdhury, T. L. Khoo, R. D. Lawson, R. K. Smither, and J. Blomqvist, *Z. Phys. A* **296**, 185 (1980).

<sup>35</sup>D. Schardt, P. O. Larsson, R. Kirchner, O. Klepper, V. T.

Koslowsky, E. Roeckl, K. Rykaczewski, K. Zuber, N. Roy, P. Kleinheinz, and J. Blomqvist, in Proceedings of the Seventh International Conference on Atomic Masses and Fundamental Constants, AMCO-7, Darmstadt, 1984, edited by O. Klepper (Technische Hochschule Darmstadt, Darmstadt, 1984) (Schriftenreihe Wissenschaft und Technik), Vol. 26, p. 222.

<sup>36</sup>K. S. Toth, Y. A. Ellis-Akovali, F. T. Avignone III, R. S. Moore, D. M. Moltz, J. M. Nitschke, P. A. Wilmarth, P. K. Lemmertz, D. C. Sousa, and A. L. Goodman, Phys. Rev. C **32**, 342 (1985).

<sup>37</sup>P. Kleinheinz, B. Rubio, M. Ogawa, M. Piiparinen, A. Plochoki, D. Schardt, R. Barden, O. Klepper, R. Kirchner, and E. Roeckl, Z. Phys. A **323**, 705 (1985).